DOI 10.1007/s10778-023-01193-2
International Applied Mechanics, Vol. 58, No. 6, November, 2022

EDGE EFFECT AND NEAR-SURFACE BUCKLING IN LAYERED COMPOSITE MATERIAL WITH IMPERFECT CONTACT BETWEEN LAYERS*

V. M. Bystrov, V. A. Dekret, and V. S. Zelens'kyi

The three-dimensional linearized theory of stability and the piecewise homogeneous medium model are used to analyze the near-surface buckling of a layered composite material in an inhomogeneous subcritical state associated with the edge effect in the vicinity of the surface load. The case of imperfect contact between layers modeled by a periodic system of interlayer cracks in the form of a mathematical cut with stress-free edges is considered. The effect of the crack size on the stress decay length, critical loads, and buckling modes is studied. A mesh-based method based on a modified variational-difference approach is used for numerical solution of the problem. The computational experiment uses the sequential and parallel algorithms of the Cholesky method to solve the system of linear algebraic equations and the subspace iteration method to solve the generalized eigenvalue problem.

Keywords: layered composite material, surface load, imperfect contact, edge effect, buckling mode, critical load, three-dimensional linearized stability theory, mesh-based method, parallel computing

Introduction. During the operation of structural members made of composite materials (CM), mechanical loads are usually directed along the reinforcement. The compressive and tensile strengths of composites are substantially different because the fracture mechanisms are different in these cases. Note that the case of compression is more difficult to predict. Compressive stresses can lead to loss of stability and fracture of either whole CM or its microstructure. The buckling of reinforcing fibers and layers is one of their possible fracture mechanisms under compression [1, 3, 12, 14, 17, 21, 27–30]. In the case of compression of unidirectional CMs by a surface load along the reinforcement, this mechanism can be a near-surface buckling in the CM structure with buckling modes decaying with distance from the surface of the CM [1, 3, 12, 14, 21]. Such a mechanism corresponds to fracture due to the crushing of the ends of samples and CM structural elements. Its study is one of the nonclassical problems of the fracture mechanics of composites [20].

The results obtained in most of these works indicate that critical loads and buckling modes depend on geometrical and mechanical factors associated with the combined effect of the CM structure and boundary conditions on the loaded surface. Under such surface loading conditions where the stress–strain state (edge effect) near the boundary surface is inhomogeneous and the stress and strain fields change substantially within the CM structure parameter (the typical length scale of CM structural inhomogeneity), the CM fracture mechanism can be associated with stress concentration [11] in the edge effect area and lead to the development of microdefects in the CM structure. Under loading conditions where the stress and strain fields change at distances that exceed the CM structure parameter, the edge effect area can be very large at certain ratios of the elastic and

S. P. Timoshenko Institute of Mechanics, National Academy of Sciences of Ukraine, 3 Nesterova St., Kyiv, Ukraine, 03057; e-mail: numer@inmech.kiev.ua. Translated from Prykladna Mekhanika, Vol. 58, No. 6, pp. 84–97, November–December 2022. Original article submitted December 28, 2021.

* The studies were sponsored by the budget program "Mathematical modeling of complex interdisciplinary processes and systems on the basis of intelligent supercomputer, grid and cloud technologies" (KPKVK 6541030).

geometric characteristics of the CM components due to the inhomogeneity and structural anisotropy of the CM, which is manifested at the meso and macro levels [5, 13, 24, 26, 31–34] and can significantly affect the critical loads and buckling modes in the CM structure [14]. Nonzero tangential shear stresses near the loaded surface, caused by the edge effect, also strongly affect the critical parameters of the CM stability [27]. Thus, the study of edge effects and buckling in the CM structure in the case of an inhomogeneous subcritical state caused by the edge effect is a complex problem of fracture mechanics, and the corresponding models for studying the CM fracture mechanisms should take into account the relation between the parameters of the decay of the edge effect and the critical parameters of CM stability [1].

The technological and operational defects and imperfections in the CM structure require modifying the approaches and models to account for their effect on the buckling in the CM structure in an inhomogeneous subcritical state associated with the edge effect near the boundary surface. In particular, this applies to the case of weakening of the adhesion between CM components due to starved spots, delamination, cracks, etc. In [32, 33], it was shown that the weakening of adhesion in the case of imperfect contact between the CM layers leads to a decrease in the decay rate and, accordingly, to an increase of the inhomogeneous stress–strain state area. The effect of this factor on the CM stability critical parameters should be studied. One of the most accurate approaches to this problem is the three-dimensional linearized theory of stability of deformable bodies (TLTSDB) [2, 18] in combination with the piecewise-homogeneous medium model. The effect of imperfect interlayer contact on the buckling in the internal structure of CM was studied based on this approach in [22, 23, 30]. There are very few studies into the near-surface buckling in the CM structure in the case of imperfect contact between the CM components.

When modeling imperfect contact between CM components, the most common approach is to use spring-layer models [15, 32], where the displacement jumps are proportional to the tangential forces along the entire contact line. The other approach is to apply perfect bonding boundary conditions at the interface between the CM components and interlayer adhesion defects of various nature [22, 23, 30]. Defects can be either cracks with stress-free edges or defects with bounded edges that correspond to slipping conditions, where the continuity condition is only satisfied by the normal displacements and stresses [10].

We will present a design model for studying the edge effect in the vicinity of the surface load of a layered CM and the near-surface buckling in the CM structure with imperfect contact between the CM layers, the contact being modeled by a system of interlayer macrocracks with stress-free edges. Macrocracks are cracks with length comparable to or exceeding the thickness of the CM reinforcement layers. We will analyze the effect of the crack size on the decay length of the edge effect, critical loads, and buckling modes in the CM structure. A multi-layer domain with symmetry boundary conditions on its sides is used as a representative element of the CM [1]. A mesh-based method based on the modified variational-difference approach [6] is used for numerical solution of the problems. The computational experiment to be performed will involve parallel computing software for solving the system of linear algebraic equations by the Cholesky method and a partial generalized algebraic eigenvalue problem for sparse symmetric matrices by the method of iterations over a subspace [9].

1. Design Model for Analyzing the Edge Effect and Near-Surface Buckling in the Structure of a Layered CM. Consider a composite material modeled by an orthotropic material in the continuum approximation. The material is under a compressive surface load acting along the layers (normally to the end surface). The study of the CM fracture mechanism is based on the following General Concept [20]: "The initial stage (start) of end-crushing fracture is near-surface buckling near the loaded end. It is necessary to take into account the possible interaction of this fracture mechanism with other fracture mechanisms. The theoretical ultimate strength in the case of near-surface fracture near the end under normal compression (end-crushing fracture) is the critical load and the critical shortening within the applied version of the TLTSDB." Due to interlayer cracks and the buckling in the CM structure under compression along the cracks, there may occur a local buckling of the material surrounding the cracks [3]. When studying CM fracture, we need to consider these mechanisms simultaneously.

The main characteristics of the design model that correspond to the General Concept and determine the problem statement for determining the critical parameters of the stability of the CM in an inhomogeneous subcritical state associated with the edge effect in the vicinity of the surface load can be stated as follows.

– the reinforcement and matrices are modeled by linear elastic isotropic bodies; such modeling can be considered acceptable for relatively short-term external loading under moderate temperatures.

– the second variant of the theory of small subcritical strains of the three-dimensional linearized theory of stability [2, 18] is applied when the initial state is determined by the geometrically linear theory; this approach is considered acceptable for relatively hard reinforced composite materials that mainly fracture under relatively small strains;

– the external loads are considered to be dead; therefore, the conditions for applying the static method of the TLTSDB (Euler's method) are satisfied; all studies are performed using the static method (bifurcation approach);

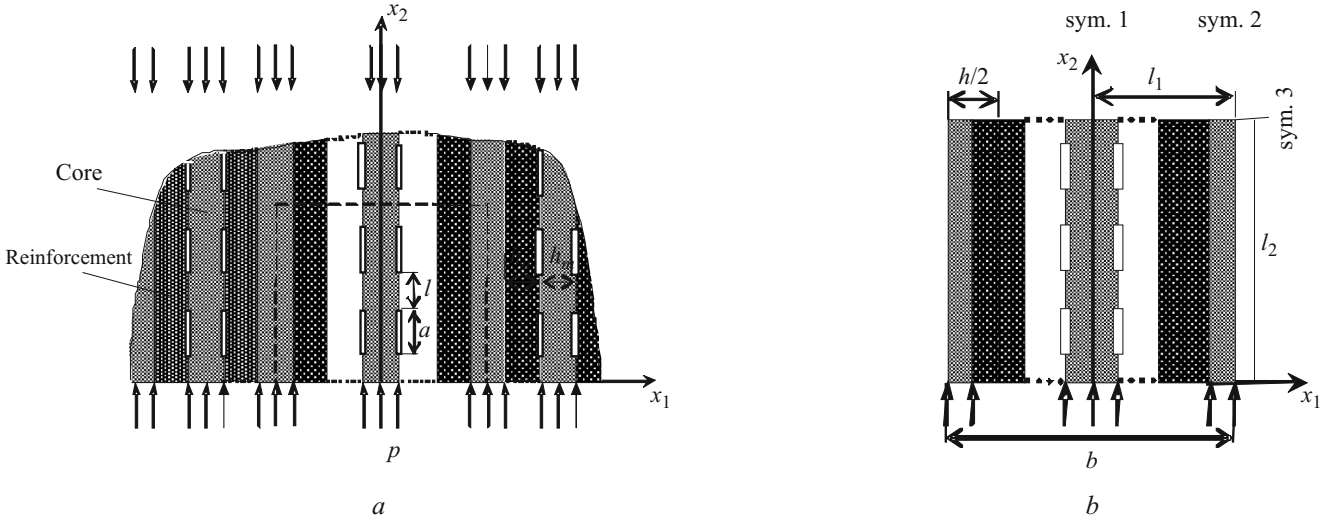

a *b*

Fig. 1

– the interface conditions between the core and the matrix are either perfect bonding (continuity of the stress and displacement vectors) or imperfect bonding (interlayer cracks) in determining the subcritical state and in solving stability problems. In the case of imperfect contact, the limiting estimates correspond to the perfect bonding of the CM layers and the perfect sliding of the layers [23] when the continuity condition is satisfied only by the normal displacements and stresses (perfectly lubricated interfaces [10]);

– the plane strain condition (longitudinal section of layered materials) is considered;

– when determining the representative element of the CM in the case of a periodic system of reinforcing elements on the sides of the design domain, conditions of periodicity or symmetry for boundary conditions can be used for problems of statics and stability; in the case of symmetry conditions, the dimensions of the design domain should be determined in a computational experiment to determine those geometrical characteristics of the domain for which the dependence of the parameters of the subcritical state and stability on the domain dimensions becomes stable with practical accuracy;

– solutions to stability problems for a representative element of the CM under boundary conditions that correspond to the symmetry conditions (rather than to the periodicity conditions) lead to higher critical loads and buckling modes that correspond to the unidirectional buckling [19];

– the area of the inhomogeneous subcritical state of the representative element is described by the parameters of the edge effect decay, including the maximum decay length of the edge effect, the geometry of the area, and the distribution of stress and strain fields in the edge effect area; these parameters are determined using a quantitative criterion of the edge effect decay [13, 26];

– the area of the inhomogeneous subcritical state for the representative element under boundary conditions that correspond to the symmetry conditions (mixed boundary conditions on the sides of the design domain) has smaller dimensions than in the case of stress-free sides [13];

– an increase in the period of the surface load during the unloading of the reinforcement layers in comparison with the parameter of the CM structure leads to an increase in the edge effect area, an increase in the wavelength of the near-surface buckling, and a decrease in its amplitude near the boundary surface and a decrease in the critical loads [1].

Figure 1*a* shows a layered CM with imperfect contact between layers and its loading conditions for studying the static edge effects in the vicinity of surface loading and near-surface buckling. Figure 1*b* shows a representative element of the material, where sym. 1, sym. 2, and sym. 3 denote the axes of symmetry $x_1 = 0, x_1 = l_1, x_2 = l_2$.

2. Problem Statement. Let us determine the decay parameters of the edge effect and solve the stability problem for a two-component CM of regular structure with imperfect contact between layers (Fig. 1*a*) uniaxially compressed along the axis Ox_2 by a surface load of constant intensity p^0. The load induces an inhomogeneous stress–strain state in the vicinity of the load (static edge effect) and has the following form:

$$p(x_1)=\sigma_{22}(x_1,0)=\begin{cases} p^0, & -h_a/2+kh\le x_1\le h_a/2+kh, \quad k=0,\pm1,\dots, \\ 0, & \text{for other } x_1, \end{cases} \tag{2.1}$$

where $h=h_a+h_m$ is the structure parameter of the layered CM; h_a, h_m are the thicknesses of the core layer (reinforcement layer) and the binding layer (matrix), respectively. We assume that at infinity, the load is applied to the reinforcement in the same way. The load does not change along the axis Ox_3. Based on the symmetry of the load and regularity of the CM structure, we solve the problems for the representative element of the material that corresponds to a design domain of finite dimensions. According to [1], the size of this domain along the axis Ox_1 corresponds to the period b of the surface load and is $l_1=b/2=8h$. The size along the axis Ox_2 is determined in a computational experiment and corresponds to constant values of the decay parameters of the edge effect with further increase in this size. Figure 1*b* shows the design domain. We believe that for such a geometry of the design domain and load conditions, the decay of the edge effect becomes stable with respect to the further increase of the load period, and the obtained results will correspond to a CM modeled by a semi-infinite domain. The edge layers of the representative element are reinforcement layers.

The design model for determining the area (decay length) of the edge effect includes a two-dimensional (plane strain) boundary-value problem of elasticity of piecewise homogeneous bodies and a quantitative criterion for determining the edge effect using the stress decay function [1, 26]. The edge effect is studied for a self-balanced load, which is a superposition of a surface load and normal stresses for a constant stress–strain state and decaying edge effect. Assuming that the core material is sufficiently hard compared to the reinforcement, we use the second variant of the theory of small subcritical strains [2, 18] when studying stability. We consider the surface load to be dead, which ensures the satisfaction of the sufficient conditions for the applicability of the static method. When using the static method, the stability problem is reduced to a generalized eigenvalue problem, in which the minimum eigenvalue μ determines the critical load, and the corresponding eigenfunction $\boldsymbol{u}=(u_1,\,u_2)$ determines the buckling mode. We consider the problem in a two-dimensional statement for the case of plane strain in the plane x_1Ox_2. Imperfect contact between layers is modeled by interlayer cracks in the form of mathematical cuts with stress-free edges.

Since the load is symmetric, the stress–strain state is determined from the following basic relations of the linear theory of elasticity for the domain $\overline{\Omega}=\{(x_1,x_2)\,|\,0\le x_1\le l_1,\,0\le x_2\le l_2\}$:

the equilibrium equation

$$\sigma^0_{ij,i}=0, \qquad x\subset\overline{\Omega}, \tag{2.2}$$

the boundary conditions

$$\sigma^0_{21}=0\wedge u^0_2=0, \qquad 0\le x_1\le l_1\wedge x_2=l_2, \qquad \sigma^0_{12}=0\wedge u^0_1=0,$$

$$(x_1=0\vee x_1=l_1)\wedge(0\le x_2\le l_2),$$

$$\sigma^0_{22}=p\wedge\sigma^0_{21}=0, \qquad 0\le x_1\le l_1\wedge x_2=0, \tag{2.3}$$

the perfect bonding conditions at the interface between the components of the CM

$$[\sigma^0_{i1}]=0,\ [u^0_i]=0, \tag{2.4}$$

the imperfect contact conditions at the interface between the central reinforcing layer and the matrix, corresponding to mathematical cuts with stress-free sides at the interface of CM components

$$\sigma^{(a)}_{i1}=0, \qquad \sigma^{(m)}_{i1}=0, \tag{2.5}$$

the relationship among stresses σ_{ij}, strains ε_{ij}, and displacements u_i within the CM component

$$\sigma^0_{ij}=\delta_{ij}A_{ik}\varepsilon^0_{kk}+2(1-\delta_{ij})G\varepsilon^0_{ij}, \qquad \varepsilon^0_{ij}=\frac{1}{2}(u^0_{i,j}+u^0_{j,i}), \qquad i\ne j, \tag{2.6}$$

where

$$A_{11} = A_{22} = \frac{E(1-\nu)}{(1+\nu)(1-2\nu)}, \quad A_{12} = \frac{E\nu}{(1+\nu)(1-2\nu)}, \quad G = \frac{E}{2(1+\nu)}, \tag{2.7}$$

A_{ij}, E, G, ν are the elastic moduli, Young's modulus, shear modulus, Poisson's ratio of the CM component.

The boundary of the domain Γ_ρ and the decay length λ_ρ of the edge effect are determined with accuracy $\rho\%$ from the following relations [26]:

$$\rho = \tilde{\rho}(x_1, x_2)|_{x \in \Gamma_\rho}, \quad \lambda_\rho = \max_{x_1, x_2 \in \Gamma_\rho} (x_2), \tag{2.8}$$

where the stress decay function $\tilde{\rho}(x_1, x_2)$ is given by

$$\tilde{\rho} = 100(\sigma_{22}^0(x) - \sigma_{\text{st}}^0) / (p(x_1, 0) - \sigma_{\text{st}}^0). \tag{2.9}$$

The function $\tilde{\rho}(x_1, x_2)$ describes the change in normal stresses in the edge effect area in comparison with the self-balanced load at the boundary $x_2 = 0$ of the design domain. In (2.9), $\sigma_{\text{st}}^0 = \sigma_{22}(x_1, l_2)$ is the constant normal stress at the boundary $x_2 = l_2$ of the design domain in the direction of the edge effect decay.

The basic equations of the TLTSDB for determining the critical parameters of CM stability are as follows:

the equations for perturbations

$$(\sigma_{ij} + \mu\sigma_{in}^0 u_{j,n})_{,i} = 0, \quad x \in \Omega, \tag{2.10}$$

the boundary conditions

$$(\sigma_{12} + \mu\sigma_{22}^0 u_{1,2}) = 0 \wedge u_2 = 0, \quad 0 \le x_1 \le l_1 \wedge x_2 = l_2,$$

$$u_1 = 0 \wedge (\sigma_{12} + \mu\sigma_{11}^0 u_{2,1}) = 0, \quad (x_1 = 0 \vee x_1 = l_1) \wedge (0 \le x_2 \le l_2),$$

$$(\sigma_{j2} + \mu p u_{j,2}) = 0, \quad 0 \le x_1 \le l_1 \wedge x_2 = 0, \tag{2.11}$$

the perfect bonding conditions between the layers

$$[\sigma_{1j} + \mu\sigma_{1n}^0 u_{j,n}] = 0, \quad [u_j] = 0, \tag{2.12}$$

the imperfect contact conditions at the interface between the central reinforcing layer and the matrix, corresponding to mathematical cuts with stress-free sides at the interface of CM components

$$\sigma_{1j}^{(a)} + \mu\sigma_{1n}^{0(a)} u_{j,n}^{(a)} = 0, \quad \sigma_{1j}^{(m)} + \mu\sigma_{1n}^{0(m)} u_{j,n}^{(m)} = 0. \tag{2.13}$$

The relationships among the perturbations of stresses σ_{ij}, strains ε_{ij}, and displacements u_i within the CM component has the form (2.6), (2.7).

The critical load is defined as

$$p_{\text{cr}} = \min|\mu| \Big/ l_1 \int_{0 \le x_1 \le l_1} p(x_1)\, dx_1 = \min|\mu|\, p^0 h_a / h, \tag{2.14}$$

where $\min|\mu|$ is the minimum (in absolute magnitude) eigenvalue of problem (2.10)–(2.13). The form of relation (2.14) shows that the compression is applied only to the reinforcement layers.

The notation in (2.10)–(2.13) is standard, and the indices change from 1 to 2 ($\wedge$, $\vee$ denote logical multiplication and addition). The superscript "0" refers to the subcritical stresses determined by solving problem (2.2)–(2.7). The index referring to the CM layer in relations (2.10)–(2.13) is omitted for convenience; in relations (2.5), (2.13), the superscript "a" to the

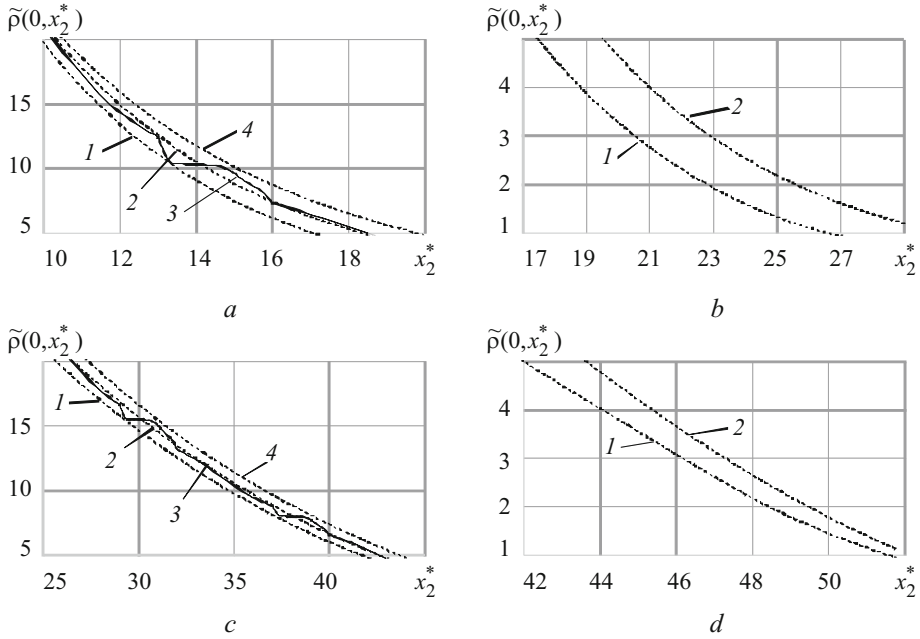

Fig. 2

reinforcement layer, while "*m*", to the matrix. In relations (2.4), (2.12), $[f(x)] = f(x-0) - f(x+0)$ is the discontinuity of the function $f(x)$.

3. Problem Solution.

3.1. Analysis of the Effect of Imperfect Contact on the Edge Effect Decay. The results obtained for the design model are shown in Fig. 1*b* for the following mechanical and geometric characteristics of CM: the ratio of Young's moduli of the reinforcement and the matrix $E_a E_m^{-1} = 100,\ 1000$; Poisson's ratios $\nu_a = \nu_m = 0.3$; macrocrack lengths $a = h, 2h, 3h$, where $h = h_a + h_m$. The size of the design domain along the axis Ox_2 determined in the computational experiment $l_2 = 20 l_1 = 160h$.

Figure 2 shows the behavior of the stress decay function $\tilde{\rho}(0, x_2^*) = \tilde{\rho}(0, x_2 / h)$ given by relation (2.9) in the reinforcement layer for the decay ranges of the edge effect $\rho = 5-20\%$ (Fig. 2*a*,*c*) and $\rho = 1-5\%$ (Fig. 2*b*,*d*): (a), (b) for $E_a / E_m = 100$; (c), (d) for $E_a / E_m = 1000$. The decay length λ_ρ of the edge effect at which the normal stress is ρ percent of the self-balanced surface load is considered equal to x_2^*. In Figs. 2*a* and 2*c*, curve *1* corresponds to perfect contact, curves *2* and *4* correspond to imperfect contact when the crack lengths $a = 2h$ and $a = 3h$. In Figs. 2*b* and *d*, curve *1* corresponds to perfect contact, curve *2* corresponds to imperfect contact when the crack length $a = 3h$. For better visualization, these dependences are shown by smoothed curves obtained by interpolation of the results. The original dependences are shown only in Fig. 2*a*,*c* for $a = 2h$ by solid lines *3*.

The figures show that when the adhesion is weakened by cracks with increasing size, the decay length of the edge effect λ_ρ increases. Thus, the decay length of the edge effect $\lambda_{\rho=5\%}$ under perfect and imperfect ($a = 3h$) contact conditions is, respectively, $17.4h$ and $19.47h$ when $E_a / E_m = 100$ and $42h$ and $43.4h$ when $E_a / E_m = 1000$.

An increase in the ratio E_a / E_m leads to an increase in the decay length of the edge effect for both perfect and imperfect contact conditions. The harder the reinforcement, the less significant this increase.

The results allow us to draw the following conclusions.

Modeling imperfect contact by applying boundary conditions at the interface sections of CM components that correspond to interlayer adhesion defects in the form of macrocracks with stress-free edges, we can study the effect of the weakening of adhesion on the decay rate of the edge effect.

Imperfect contact and weakened adhesion when the size of macrocracks increases lead to an increase in the decay length of the edge effect, and it decays more slowly.

3.2. Analysis of the Effect of Imperfect Contact on the Critical Loads and Buckling Modes. The results obtained for the design model are shown in Fig. 1*b* for the following mechanical and geometric characteristics of CM: the ratios of Young's

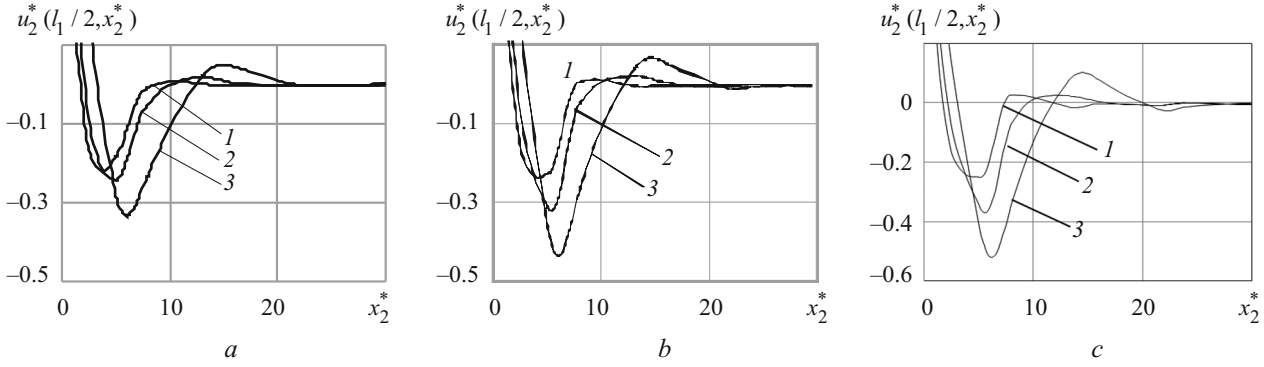

Fig. 3

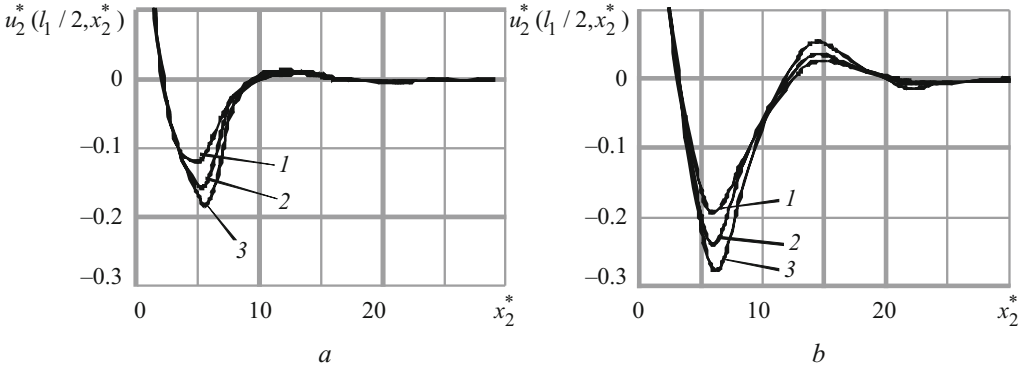

Fig. 4

moduli of the reinforcement and the matrix $E_a E_m^{-1} = 50, 100, 500$; Poisson's ratios $\nu_a = \nu_m = 0.3$; macrocrack lengths $a = h, 2h, 3h$. The size of the design domain along the Ox_2-axis $l_2 = 20l_1 = 160h$.

Figures 3 and 4 show the buckling modes $u_2^*(l_1/2, x_2^*) = u_2(l_1/2, x_2/h)/u_2^{\max}$ in the cross-section $x_1 = l_1/2$ of the middle reinforcement layer of the CM representative element, where $u_2^{\max}$ is the maximum displacement perturbation in this cross-section. The curves show the dependence of the buckling modes on the macrocrack size a and the ratio E_a / E_m. Figure 3 shows the near-surface buckling modes in the middle reinforcing layer of the CM representative element for perfect contact (Fig. 3*a*), in the presence of interlayer cracks of size $a = 2h$ (Fig. 3*b*) and size $a = 3h$ (Fig. 3*c*) for different values of E_a / E_m: 50 (curve *1*), 100 (curve *2*), 500 (curve *3*). Figure 4 shows near-surface buckling modes in the middle reinforcing layer of the CM representative element for $E_a / E_m = 100$ (Fig. 4*a*) and $E_a / E_m = 500$ (Fig. 4*b*) under different contact conditions: perfect contact (curve *1*); interlayer cracks of size $a = h$ (curve *2*); interlayer cracks of size $a = 2h$ (curve *3*).

The buckling modes are wave-like with amplitude decreasing with distance the loaded boundary surface of the CM. The presence of cracks and increase in their length slow down the decrease in the amplitude, and the harder the reinforcement, the more intensive the decrease.

Figure 5 shows the dependence of the critical loads for perfect and imperfect contacts between the reinforcement layers and the matrix on the ratio E_a / E_m for different values of the macrocrack size a: perfect contact (curve *1*); interlayer cracks of size $a = h$ (curve *2*), $a = 2h$ (curve *3*), $a = 3h$ (curve *4*).

Imperfect contact between the CM layers and the increase in the crack size leads to a decrease in the critical loads and affects the critical loads to a greater extent compared to the perfect contact at higher values of E_a / E_m.

Imperfect contact and an increase in the crack size lead to an increase in the inhomogeneous stress state area in the vicinity of the surface load and a corresponding increase in the decay length of the buckling modes as their amplitude increases.

4. Numerical Solution and Computational Algorithm. The problems of determining the subcritical state based on relations (2.2)–(2.7) and the problem of determining the critical parameters of CM stability (2.10)–(2.14) are solved using a mesh-based method and the concept of reference scheme. Using this approach, the difference scheme for the design domain is

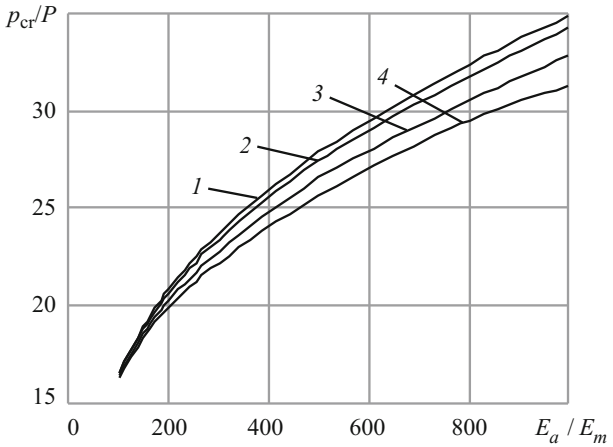

Fig. 5

developed at each mesh node as a certain sum of the values of the reference scheme, which is a difference scheme obtained by the variational-difference method for the difference mesh cell template [6].

When numerically solving the problem using the mesh-based method, an inhomogeneous difference grid is introduced in the design domain $\overline{\Omega}$ consisting of a set ω of internal nodes and a set γ of boundary nodes and nodes at the contact of the CM components, and problems (2.2)–(2.7), (2.10)–(2.13) correspond to the solution of a system of linear algebraic equations (SLAE) and an algebraic eigenvalue problem with sparse symmetric positive definite matrices. These problems are as follows:

$$Au^0 = \Phi, \quad x \in \overline{\omega}, \tag{4.1}$$

$$Au = \lambda Bu, \quad x \in \overline{\omega}, \tag{4.2}$$

where u^0 and u are the column vectors of displacement and perturbation values at the nodes of the difference mesh $\overline{\omega}$; Φ is the column vector of mass forces at nodes ω and surface forces and displacements at nodes $x \in \gamma$ according to the boundary conditions (2.3), (2.11), the perfect contact conditions between the CM layers (2.4), (2.12), and the imperfect contact conditions (2.5), (2.13). The matrices A, B are adjusted so as to account for the boundary conditions for the displacements [6]. The imperfect contact between the CM layers corresponds to homogeneous boundary conditions for stresses in each CM component.

According to the concept of reference schemes [6], the matrices A, B, and the vector of the right-hand sides Φ of problems (4.1), (4.2) are obtained by summing the matrices A^q, B^q and vectors Φ^q corresponding to the difference schemes on the cell of the difference mesh $\overline{\omega}$, in all cells $q = \overline{1,Q}$:

$$A = \sum_{q=1}^{Q} A^q, \quad A^q = (A_{ij}^q)_{2\times 2},$$

$$B = \sum_{q=1}^{Q} B^q, \quad B^q = (B_{ij}^q)_{2\times 2},$$

$$\Phi = \sum_{q=1}^{Q} \Phi^q, \quad \Phi^q = (\Phi_1^q, \Phi_2^q)^T. \tag{4.3}$$

The expressions for the difference operators and corresponding matrices of the algebraic problems can be found in [14, 16]. Numerical methods are used to solve discrete problems according to the procedure from [4, 16]. In this case, the direct Cholesky method was used to determine the initial state when solving the system of linear algebraic equations, and the subspace iteration method was used to determine the critical stability parameters when solving the generalized eigenvalue problem. As part of the computational experiment, sequential [7] and parallel [9] algorithms of these methods were applied.

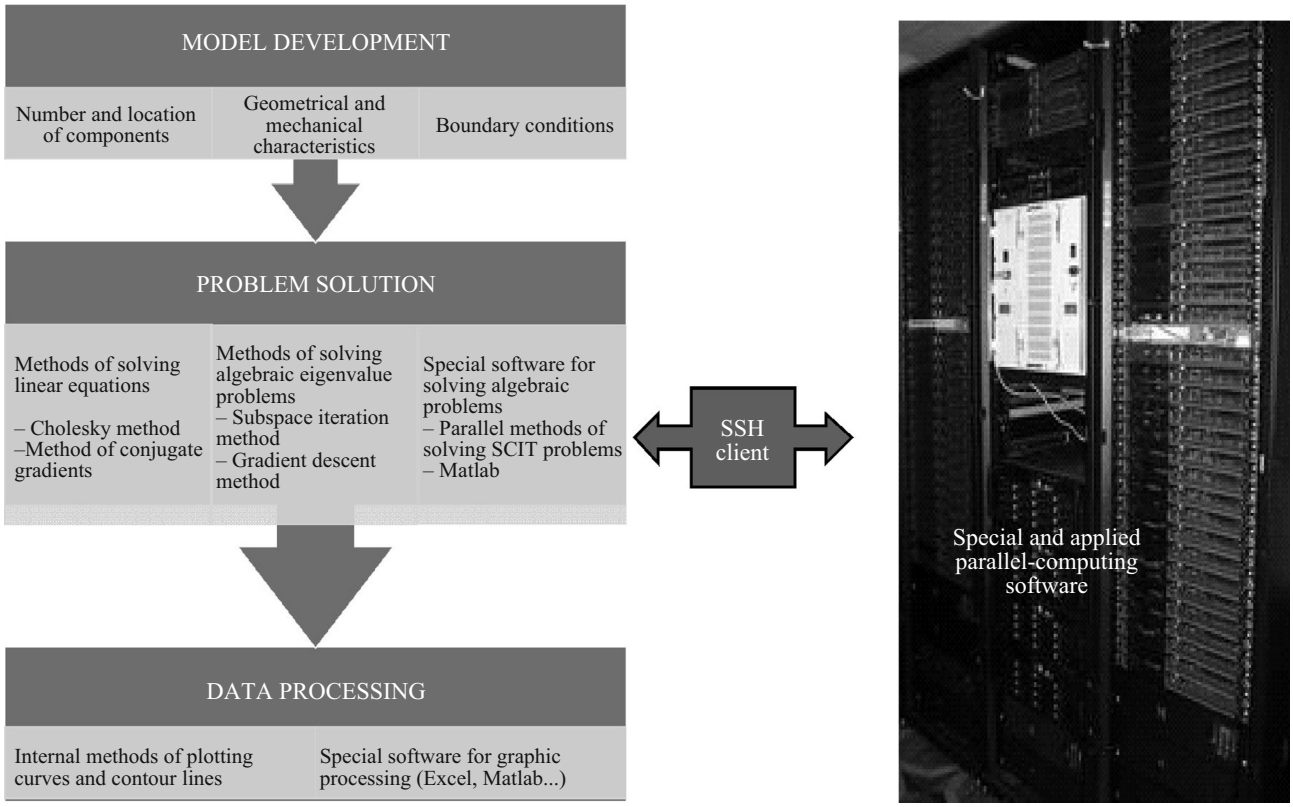

Fig. 6

An algorithm for the numerical analysis of the subcritical state and stability of reinforced CM was designed to perform calculations in a computing environment that includes a local PC and a supercomputer connected via the Internet. Figure 6 shows the components of the computing environment. These components are problem-oriented computing applications [4] on the local PC and data preparation and processing of calculated results on the SCIT supercomputer [8], SSH clients for allocation of computing resources (PuTTY [35]), and data exchange (WinSCP [36]) between the local PC and the supercomputer, special software [9] for parallel computing on the supercomputer.

A discrete model is created on the local PC and the solution convergence of discrete problems is studied within the computational experiment. The necessary computational resources for the conventional or parallel computers to obtain solutions with required accuracy are determined. Based on the computational experiment results on the local PC, small-scale problems are solved using sequential algorithms for solving SLAE and the algebraic eigenvalue problem, and data are preprocessed for transmission to the appropriate computing node of the supercomputer for parallel calculations.

Thus, the computational algorithm for determining the initial state and the edge effect decay parameters (2.2)–(2.9) and the stability problem (2.10)–(2.14) in the computing environment includes the following stages:

– development of the discrete problem (4.1), (4.2) regarding the formation of the matrix A and vector Φ according to relation (4.3) and preprocessing of data on the necessary representation of the matrix A and vector Φ for their transmission to the supercomputer for parallel calculations;

– solving the system of algebraic equations corresponding to the difference problem (4.1) based on the sequential or parallel algorithm of the Cholesky method;

– calculation of the stress components σ_{ij}^0 and edge effect decay parameters based on the obtained values of the displacement components u_i^0 according to the discrete analog of relations (2.6)–(2.9), development of the discrete model regarding the formation of the matrix B according to relations (4.3) and preprocessing of data on the required representation of the matrix B for parallel calculations;

– solving the algebraic eigenvalue problem corresponding to the difference problem (4.2) on the basis of the sequential or parallel algorithm of the subspace iteration method and calculation of the critical loads according to (2.14).

In this paper, the calculations were performed on the computing node of the SCIT supercomputer [8] (one computing node, two octa-core processors of the Xeon E5 2600 series, 2 GPU Tesla M2075). The efficiency of the applied algorithm is comparable to that for the numerical analysis of the stability of CM reinforced with short fibers [16, 25].

Conclusions. The results of the calculation allow us to draw the following conclusions.

The design model based on TLTSDB and the piecewise-homogeneous medium model, when a multi-layered design domain with boundary conditions on its sides that satisfies the symmetry conditions is used as a representative element of CM, allows us to study the end-crushing fracture mechanism in samples and structural members made of layered CM taking into account the imperfect contact between the layers.

Modeling of the imperfect contact by applying boundary conditions at the interface of CM components, which correspond to interlayer adhesion defects in the form of macrocracks with stress-free edges, allows us to study the effect of the weakening of adhesion on the decay rate of the edge effect, critical loads, and buckling modes in the CM structure.

Weakening of interlayer adhesion due to interlayer cracks and increase in their length lead to a decrease in the decay rate of the edge effect, an increase in the amplitude of the buckling modes in the vicinity of the surface load, and their slower decay with distance from the surface. The harder the reinforcement, the stronger this effect.

Weakening of interlayer adhesion due to interlayer cracks and increase in their length lead to a decrease in the critical loads and affects this decrease to a greater extent in the case of harder reinforcement.

Thus, the weakening of interlayer adhesion leads to an increase in the effect of the inhomogeneous subcritical state on the critical parameters of CM stability, a decrease in CM strength, and their failure due to the near-surface buckling in the CM structure under reduced critical loads.

In mathematical modeling of stability problems of reinforced CM, the use of parallel algorithms for solving systems of linear algebraic equations and algebraic eigenvalue problems based on supercomputer technologies allows us to solve discrete problems of large dimensions with effective use of computing resources and with required accuracy.

REFERENCES

1. V. M. Bystrov, "Edge effect and near-surface buckling in a layered composite material under surface compressive load," *Dop. NAS of Ukraine*, No. 10, 29–37 (2019).
2. A. N. Guz, *Fundamentals of the Three-Dimensional Theory of Stability of Deformable Bodies* [in Russian], Vyshcha Shkola, Kyiv (1986).
3. A. N. Guz, *Fundamentals of the Fracture Mechanics of Compressed Composites*, the two-volume series (Vol. 1, *Structural Failure of Materials* and Vol. 2, *Related Fracture Mechanisms*) [in Russian], Litera, Kyiv (2008).
4. A. N. Guz and V. A. Dekret, *Short-Fiber Model in the Theory of the Stability of Composites* [in Russian], LAP Lambert Acad. Publ., Saarbrücken (2015).
5. V. T. Golovchan (ed.), *Statics of Materials*, Vol. 1 of the 12-volume series *Mechanics of Composite Materials* [in Russian], Naukova Dumka, Kyiv (1993).
6. Ya. M. Grigorenko, Yu. N. Shevchenko, A. T. Vasilenko, et al., *Numerical Methods*, Vol. 11 of the 12-volume series *Mechanics of Composite Materials* [in Russian], A.S.K., Kyiv (2002).
7. S. Pissanetzki, *Sparse Matrix Technology* [in Russian], Mir, Moscow (1988).
8. http://icybcluster.org.ua/
9. A. N. Khimich, I. N. Molchanov, A. V. Popov, T. V. Chistyakova, and M. F. Yakovlev, *Parallel Algorithms for Solving Problems of Computational Mathematics*, Naukova Dumka, Kyiv (2008).
10. J. Aboudi, "Damage in composites-modelling of imperfect bonding," *Compos. Sci. Technol.*, **28**, No. 2, 103–128 (1987).
11. I. V. Andrianov, V. V. Danishevs'kyy, and D. Weichert, "Analytical study of the load transfer in fiber-reinforced 2D composite materials," *Int. J. Solids Struct.*, No. 45, 1217–1243 (2008).
12. M. A. Biot, "Edge buckling of laminated medium," *Int. J. Solids Struct.*, **4**, No. 1, 125–137 (1968).
13. V. M. Bystrov, V. A. Dekret, and V. S. Zelenskii, "Numerical analysis of the edge effect in a composite laminate with compressed reinforcement plies," *Int. Appl. Mech.*, **51**, No. 5, 561–566 (2015).
14. V. M. Bystrov, V. A. Dekret, and V. S. Zelenskii, "Loss of stability in a composite laminate compressed by a surface load," *Int. Appl. Mech.*, **53,** No. 2, 156–163 (2017).

15. Z. Cheng, D. Kennedy, and W. F. Williams, “Effect of interfacial imperfection on buckling and bending behavior of composite laminates,” *AIAA J.*, **34**, No. 12, 2590–2595 (1996).
16. V. A. Dekret, V. M. Bystrov, and V. S. Zelenskiy, “Numerical analysis of the buckling of near-surface short fibers in a weakly reinforced composite material,” *Int. Appl. Mech.*, **57**, No. 11, 687–699 (2021).
17. N. A. Fleck, “Compressive failure of fiber composites,” *Adv. Appl. Mech.*, No. 33, 43–117 (1997).
18. A. N. Guz, *Fundamentals of the Three-Dimensional Theory of Stability of Deformable Bodies*, Springer-Verlag Heilberg, Berlin (1999).
19. A. N. Guz, “Stability of elastic bodies under uniform compression. Review,” *Int. Appl. Mech.*, **48**, No. 3, 241–293 (2012).
20. A. N. Guz, “Nonclassical problems of fracture/failure mechanics: on the occasion of the 50th anniversary of the research (review) II,” *Int. Appl. Mech.*, **55**, No. 3, 239–295 (2019).
21. A. N. Guz and Yu. V. Kokhanenko, “Numerical solution of three-dimensional stability problems for elastic bodies,” *Int. Appl. Mech.*, **37**, No. 11, 1369–1399 (2001).
22. I. A. Guz, “Plane problem of the stability of composites with slipping layers,” *Mech. Compos. Mater.*, **27**, No. 5, 547–551 (1991).
23. I. A. Guz, “Composites with interlaminar imperfections: substantiation of the bounds for failure parameters in compression,” *Compos. Part B*, **29**, No. 4, 343–350 (1998).
24. C. O. Horgan and L. A. Carlsson, “Saint-Venant end effects for anisotropic materials,” *Compr. Compos. Mater. II*, No. **7**, 38–55 (2018).
25. A. N. Khimich, V. A. Dekret, A. V. Popov, and A. V. Chistyakov, “Numerical study of the stability of composite materials on computers of hybrid architecture,” *J. Aut. Inform. Sci.*, **50**, No. 7, 7–24 (2018).
26. Yu. V. Kokhanenko and V. M. Bystrov, “Edge effect in a laminated composite with longitudinally compressed laminas,” *Int. Appl. Mech.*, **42**, No. 8, 922–928 (2006).
27. M. D. Nestorovic and N. Triantafyllidis, “Onset of failure in finitely strained layered composites subjected to combined normal and shear loading,” *J. Mech. Phys. Solids.*, No. 52, 941–974 (2004).
28. C. R. Schultheisz and A. M. Waas, “Compressive failure of composites. Part 1: testing and micromechanical theories,” *Progr. Aerosp. Sci.*, No. 32, 1–42 (1996).
29. C. Soutis and I. A. Guz, “Predicting fracture of layered composites caused by internal instability,” *Comp. Part A.: App. Scien. Man.*, **39**, No. 9, 1243–1253 (2001).
30. C. Soutis and I. A. Guz, “Fracture of layered composites by internal fibre instability: Effect of interfacial adhesion,” *Aeronout J.*, **110**, No. 1105, 185–195 (2006).
31. N. Tullini and M. Savoia, “Decay rates for Saint-Venant end effect for multilayered orthotropic strip,” *Int. J. Solids Struct.*, **34**, No. 33, 4263–4280 (1997).
32. N. Tullini, M. Savoia, and C. O. Horgan, “End effect in multilayered strips with imperfect bonding,” *Mech. Mat.*, **26**, No. 1, 23–34 (1997).
33. A. C. Wijeyewickrema and L. M. Keer, “Axial decay of stresses in a layered composite with slipping interfaces,” *Comp. Eng.*, **4**, No. 9, 895–899 (1994).
34. A. C. Wijeyewickrema, “Decay of stresses induced by self-equilibrated end loads in a multilayered composite,” *Int. J. Solids Struct.*, **32**, No. 3/4, 515–523 (1995).
35. https://www.chiark.greenend.org.uk/~sgtatham/putty/
36. https://winscp.net/eng/index.php